# Re-exploring the inflammation-related core genes and modules in cerebral ischemia

**Wenjing Lv**
The Affiliated Hospital of Qingdao University
**Junqi Jiang**
Qingdao University
**Yi Xu**
Qingdao University
**Zhiyuan Chen**
Qingdao University
**Zixuan Wang**
The Affiliated Hospital of Qingdao University
**Ang Xing**
The Affiliated Hospital of Qingdao University
**Xueping Zheng**
The Affiliated Hospital of Qingdao University
**Tingting Qu**
The Affiliated Hospital of Qingdao University
**Qi Wan** ( qwanwh@hotmail.com )
Qingdao University https://orcid.org/0000-0001-6014-1620

**Research Article**

**Keywords:** Brain Ischemia, Reperfusion Injury, Inflammation, Thrombo-inflammation

**Posted Date:** March 24th, 2022

**DOI:** https://doi.org/10.21203/rs.3.rs-1470032/v1



**Version of Record:** A version of this preprint was published at Molecular Neurobiology on March 3rd, 2023. See the published version at https://doi.org/10.1007/s12035-023-03275-1.

## Abstract

The genetic transcription profile of brain ischemic and reperfusion injury remains elusive. To address this, we used an integrative analysis approach including differentially expressed genes (DEGs) analysis, weighted-gene co-expression network analysis (WGCNA), and pathway and biological processes analysis to analyze data from the microarray studies of nine mice and five rats after middle cerebral artery occlusion (MCAO), and six primary cell transcriptional datasets in the Gene Expression Omnibus (GEO). We identified reperfusion as the main confounding factor in gene profile changes. Our analyses of pathway and biological processes revealed upregulated functional modules involved in inflammatory disequilibrium and thrombus formation. Astrocytes, microglia, and macrophages were the main contributors of inflammation-related gene changes. Novel core hubs implicated in negative regulation of inflammation (Zfp36, Nfkbiz, and Maff) were identified and validated. Collectively, these results expand our knowledge of the genetic profile involved in brain ischemia and reperfusion, highlighting the crucial role of inflammatory disequilibrium in brain ischemia.

## Background

Stroke is a leading cause of death and disability worldwide, and approximately 80% of strokes are caused by cerebral ischemia [1]. Approximately 70% of ischemic strokes are caused by the occlusion of a major cerebral artery [2]. The mainstay of acute treatment for ischemic stroke is rapid recanalization via thrombolysis or mechanical thrombectomy. However, such treatments must be administered only within a narrow therapeutic window [3]. Even after successful recanalization, infarcts often continue to increase in size, a process referred to as ischemia-reperfusion injury. In cases of unsuccessful recanalization, the primary vessel occlusion persists [4]. Several clinical trials have attempted to improve the outcome after an ischemic stroke, including antioxidant strategies, neuronal protective strategies, and anti-inflammatory strategies, but most of these approaches have failed. Thus, this highlights the critical need for developing new understandings of the mechanisms underlying ischemic stroke [5].

It is a challenge to obtain human brain samples from ischemia stroke patients. As an alternative, the middle cerebral artery occlusion (MCAO) model has been used as the primary model in stroke research. The transient MCAO model, which mimics stroke with reperfusion, represents 2.5%–11.3% of large vessel stroke patients, while permanent MCAO or gradual transient MCAO mimics a stroke without recanalization, representing the majority of stroke patients [6].

We analyzed transcriptome datasets from MCAO to identify differentially expressed genes (DEGs) for biological function analysis. The application of bioinformatic tools allows improved identification of altered pathways and hub-genes, enabling us to explore new targets of brain ischemia. We validated the unreported hub-genes in vivo and further re-evaluated the network and function of hub-genes in transcriptome datasets of primary cells (Figure 1A).

## Results

### Meta-analysis of brain ischemia microarray datasets

We conducted a meta-analysis of gene expression microarray datasets of MCAO according to the guidelines put forth by Ramasamy [7]. Microarray data of 131 mouse brain tissue samples (71 MCAO and 60 controls) from the GEO database were analyzed as training datasets (DS1) (Table S1). For each sample, the characteristics of treatment, sampling site, ischemia time, and reperfusion time were collected.

We identified 2669 DEGs between groups (adj. $p$<0.05). The upregulated DEGs were more significant and pronounced than the downregulated DEGs (Figure 1B, Table S2). Supervised hierarchical clustering based on DEGs showed distinct clustering of the majority of MCAO samples, and the clustering was independent of sampling sites, ischemia time, and reperfusion time (Figure 1C). Among all MCAO samples, 13 samples with 24-h reperfusion time showed stronger variations compared to controls and other MCAO samples (Figure 1C).

To test whether these findings were replicable, we analyzed the microarray data from 101 rat brain samples in the GEO datasets. Supervised hierarchical clustering based on the rat DEGs (adj. $p$<0.05) showed poor clustering of MCAO samples and controls (Figure S1B), indicating that integrated data from rat samples have poorer reliability compared with mouse samples. We chose 39 samples from five rat GEO series with more condensed clustering (20 controls and 19 MCAO) as the validation datasets (DS2, Table S1). There were 564 increased DEGs and 677 decreased DEGs in DS2 (adj. $p<0.05$). Because of the larger size, we adjusted the statistical criteria to adj.$p$ < 0.01 in DS1, and the DEGs in DS1 showed good replicability with the DEGs in DS2 (Figure 1D). Moreover, Atf3, Timp1, Cd14, Lgals3, Hmox1, Ccl2, Emp1, Ch25h, Hspb1, Adamts1, Cd44, Icam1, Anxa2, Rgs1, and Vim showed significant increases in both DS1 and DS2 (Figure 1E, Table S3). Hierarchical clustering of DS2 samples based on either DS2-DEGs or the overlapped DEGs showed distinct separation of MCAO and controls (Figure S1C). In addition, hierarchical clustering of DS1 samples based on the overlapped DEGs showed distinct clustering of the majority of MCAO samples (Figure S1A), similar to the clustering observed in DEGs in DS1 (Figure 1C). Thus, differentially expressed analysis produced robust and highly reproducible results, warranting further analysis.

### WGCNA analysis identified ischemia and reperfusion relevant modules

Next, we applied weighted-gene co-expression network analysis (WGCNA) based on DEGs (adj. $p$<0.05) in DS1 to integrate the expression differences into a higher order systems level context. The expression levels of each module were summarized by the first principal component (the module eigengene). We identified nine modules by clustering of module eigengenes (Figure 2A; Figure S1D). The relationship of the module eigengene to sample characteristics provided a complementary assessment of potential confounder variables (Figure 2B). Modules were highly correlated with treatment but were not significantly related to the sampling sites (Figure 2B). We used Pearson correlation coefficients to reassess the correlation between the two most highly ranked positive or negative modules and treatment type and found that the blue, turquoise, brown, and purple modules had significant correlations with treatment type (Figure S1E).

The DEGs in DS1 had 24 genes that were known human stroke susceptibility genes [8] [9] [10] (Table S9). Remarkably, the blue and turquoise modules had 19 of 24 genes (Table S9). Therefore, genes in the DS1-blue and turquoise modules were most likely to map the molecular changes in human stroke. The correlations of modules with ischemia time and reperfusion time were similar with that with groups, and this was due to the confounding effects from controls. We further analyzed the module eigengenes of 71 MCAO samples (Figure S2A, C) and identified reperfusion time as a main factor associated with gene profile changes. Among the reperfusion time related modules, the turquoise module genes increased with prolonged reperfusion time, while the green module genes decreased (Figure S2B, D). Of the 885 genes in the DS1-turquoise module, 761 of them increased with prolonged reperfusion time (P = 5.2E-176, Figure 2C).

Genes associated with Alzheimer's disease (AD) play a key role in brain damage due to ischemia and reperfusion [11]. The DEGs from a gene expression dataset of frontal and temporal cortex tissues in AD (GSE122063) showed highly significant overlap with DEGs in DS1 (Figure S3A). Among the four modules relevant to ischemia, the turquoise module had a significant overlap with increased DEGs in AD (Figure S3B).

### Functional analysis and hub-gene identification of inflammation-related blue module

The blue module eigengene was highly expressed in MCAO cases, indicating that the genes in this module are upregulated in the MCAO brain (Figure S3C). Most genes did not increase with reperfusion time; indeed, some even decreased (Figure 2C). We therefore speculated that the genes in the blue module may play a priming role in subsequent complex molecular events. We applied GSEA and GSVA analyses to the genes in DS1 and metascape analysis to the module genes. The overlaps of the three analysis methods were regarded as the pathways and biological processes that the separate module genes involved (Figure 1A). Genes in the blue module were implicated in the inflammation process (including T-cell differentiation, vasculature development, cytokine-cytokine receptor interaction, and tissue morphogenesis), hydrolase and peptidase activity, MAPK signaling pathway, and apoptotic signaling pathways (Figure 3A, Table S5). All involved pathways and processes were upregulated in brain ischemia (Figure 3A). Cell type-specific markers (including neurons, astrocytes, mixed microglia, oligodendrocytes, and macrophages) were used to assess the cell contribution to the module gene profile [12] [13]. No significant enrichment markers were detected in the blue module (Table S4). We further analyzed the RNA data from *ex vivo* inflammation associated primary cells in brain ischemia models from GEO datasets, including microglia, astrocyte, epithelium cell, and macrophages (Table S1). The genes in the blue module showed significant overlap with astrocyte-relevant DEGs ($p$ = < 0.0001) and microglia-relevant DEGs ($p$= 0.007, Table S4), indicating that gene changes in the blue module may be dominated by astrocytes and microglias.

A further advantage of network analysis over differential expression (DE) analysis is that it allows the inference of the functional relevance of genes based on their network position. In this case, the hubs had the highest rank of the module membership. The core hubs of the blue module are listed in Table S6. One gene in particular, Icam1, is a known stroke susceptibility gene and is involved in the inflammation process [10]. Four of the hubs were never been reported in brain ischemia, including Zfp36, Rhoj, Maff, and Nfkbiz (Figure 5). Twenty of the 21 hub-genes were detected as DEGs in primary astrocytes (Figure 4A, B, Table S7). We further explored the protein-protein interaction (PPI) network of core hubs and known human stroke susceptibility genes in the STRING database and found that the genes most strongly connected to stroke susceptibility genes were Adamts1, Zfp36, Nfkbiz, Ccl2, and Hmox1 (Figure 4C). The transcriptions of Zfp36, Rhoj, Maff, and Nfkbiz in DS1 rapidly increased as early as 2 h after reperfusion and lasted at least 24 h (Figure S5).

### Turquoise module is a thrombo-inflammation-related module involved in reperfusion injury

The turquoise module eigengene showed high expression in MCAO cases, indicating that genes were upregulated in the MCAO brain and increased with reperfusion time (Figure S3C, 2C). The turquoise module showed markers of mixed microglia (60% microglia, 40% astrocyte and oligodendrocyte), and its genes, including core hubs, showed high significant overlap with DEGs of primary astrocytes and microglia (Table S4, S7). The pathway enriched in the turquoise module was involved in two main processes of thrombo-inflammation [14]. The first was leukocyte activation and migration related molecular events, such as actin filament-based processes, integrin pathways, and extracellular matrix organization. The second was platelet activation and degranulation by the transmembrane receptor protein tyrosine-kinase signaling pathway [15] (Figure 3C, Table S5). This suggests that platelet activation and inflammatory responses are concomitant in ischemia–reperfusion in acute stroke. The core hubs of the turquoise module are listed in Table S6, including Tnc as an astrocyte marker and Tgfbi as a macrophage marker. Mmp3 and Serpina3n, are homologues of the known human stroke susceptibility gene MMP12 and Serpine1, respectively. Serpina3n, Ms4a6d, and Tgfbi have never been reported in brain ischemia, and their transcription remarkably increased from 8 h and peaked at 24 h following stroke (Figure S5). Serpina3n, Lgals3, Mmp3, Vim, Cd44, Spp1, and Tgm2 showed interactions with established human stroke susceptibility genes in the STRING database (Figure 4C).

### Brown and purple module genes were decreased in MCAO

The brown module of co-expressed genes was negatively related to ischemia status, showing decreases after stroke (Figure S3C), and it was enriched for oligodendrocyte markers (Table S4). This module, which was downregulated in the MCAO brain, showed activity in response to oxidative stress, porphyrin metabolic processes, and synapse transport (Figure S4C, 3B). Another decreased module was the purple module (Figure S3C), whose genes have been implicated in response to hormone and neurotransmitter transport (Figure 3D, S4D). The unreported core hubs—Gpr34, Myoc, Crybb1, Rhobtb2, and Rgs9—decreased in transcription processes to the lowest point at 24 h after stroke (Figure S5).

### Expression identification of core hubs

We validated the transcription of unreported hub-genes. Zfp36 mRNA was upregulated in permanent MCAO; Rhoj, Nfkbiz, Ms4a6d, and Serpina3n mRNAs were upregulated in both transient MCAO and permanent MCAO; Rgs9 mRNA was downregulated in transient MCAO; and Gpr34 mRNA was downregulated in permanent MCAO (Table 1). We further quantitated Nfkbiz, Zfp36, Maff, Rhoj, and Tgfbi proteins in both permanent and transient MCAO. Nfkbiz, Zfp36, Tgfbi,

and Maff proteins were upregulated in permanent MCAO, but not in transient MCAO. Therein, Tgfbi protein signals were fuzzy, which might indicate that it is less abundant in the brain. Rhoj protein remained unchanged in both permanent and transient MCAO (Figure 5).

Several hub-genes have been previously identified as being human stroke-associated genes. The polymorphisms of Adamts-1 (rs416905 and rs402007) have been found to be associated with ischemic stroke caused by large artery atherosclerosis (LAA) in humans, and it is upregulated in unstable carotid plagues and the ischemic brain [16-18]. Galectin-3 (encoded by Lgals3) is a mediator of microglia responses in the injured brain [19]. IL-10-STAT3-Galectin-3 axis is essential for osteopontin (encoded by Spp1)-producing reparative macrophage polarization [20], and both Galectin-3 and osteopontin are emerging biomarkers in stroke, responsible for monitoring brain microglial activation [21] [22]. We found Adamts-1, Lgals3, and Spp1 mRNA upregulation in both permanent and transient MCAO mouse, pointing to potential shared mechanisms of stroke between species.

## Discussion

In this study, an integrated analysis of mRNA expression after brain ischemia was performed using eight publicly available mouse GEO datasets, five rat GEO datasets, and primary cells. We found suggestive evidence of the MAPK signaling pathway, apoptosis, and an increase in thrombo-inflammation, which were reported in previous studies. Additionally, in this integrated analysis of experimental animals, we reported and validated novel negative regulators of inflammation, including Zfp36, Nfkbiz, and Maff, as core hub-genes after ischemia, which provided suggestive targets for further inflammatory studies in stroke.

Zfp36 is a global post-transcriptional regulator of feedback control in inflammation, promotes cell quiescence, and inhibits apoptosis [23] [24]. It is an RNA-binding protein involved in mRNA metabolism pathways, and it contains two tandemly repeated CCCH-type zinc-finger motifs, binds to AU-rich elements (AUUUA) in the 3′-untranslated regions of specific mRNA, and leads to target mRNA decay [25]. It degrades Tnf, Ptgs2, and Ccl3 mRNAs and negatively regulates NF-κB signaling at the transcriptional corepressor level [26] [27] [28] [29]. Recently, Zfp36 was reported to be increased in immortalized hippocampal HT22 neuronal cells after oxygen-glucose deprivation/reoxygenation treatment, and it protects against mitochondrial fragmentation and neuronal apoptosis [30]. In our mouse MCAO models, Zfp36 was upregulated in permanent MCAO, but not in transient MCAO; thus, we speculate that study on the regulation of inflammation by Zfp36 after brain ischemia may be a promising future research direction.

IkappaB-zeta (encoded by Nfkbiz) is the last identified member of IkappaB family proteins, and it is strongly induced upon stimulation by LPS, which stimulates cells through the Toll-like receptor 4, IL1-β, and IFN-γ, and localizes in the nucleus, where it inhibits P65 activity [31,32]. Transcription of Nfkbiz is dose-dependent in fibroblast, and it only mediates the transcriptional response to TNF and IL-17A, but not TNF alone [33]. It also controls macrophage IL-10 expression [34]. Emerging evidence indicates that NKT cells accumulate in the ischemic hemisphere at 24 and 48 h after ischemia, while the role of different NK cell subsets is unclear [35]. We found an increased amount of Th1-type cytokines, such as IL10, and Th2-type cytokines, such as IFNr, after ischemic stroke. The regulation of Nfkbiz by Th1 and Th2 cells after brain ischemia will be an interesting direction for future research.

Maff belongs to the small Maf proteins (sMafs), which are basic leucine zipper (bZIP)-type transcription factors. It forms homodimers by themselves and heterodimers with p45 NF-E2, Nrf1, Nrf2, and Nrf3. Homodimers act as transcriptional repressors, while heterodimers are transcriptionally active; this depends on its heterodimeric partner molecules and context [36]. Recent studies revealed that Maff regulates an atherosclerosis relevant network connecting inflammation and cholesterol metabolism [37]. There are no reports about its inflammation regulation after stroke.

$Ser^{232}$ and $Ser^{235}$ phosphorylation in Ms4a6d leads to the activation of JAK2-STAT3-A20 cascades, which further results in nuclear factor κB suppression and *Nlrp3* and *Il-1*β repression [38]. We did not revalidate its protein levels due to the lack of commercial antibodies. It will be an interesting investigation target in stroke.

AD is a chronic inflammatory neurodegenerative disease in which the brain undergoes an innate immune response, including large changes in the phenotypes of microglia and astrocytes, and disruptions to the blood-brain barrier (BBB) [39]. The turquoise module showed significant overlap with increased DEGs in AD (Figure 2C). Indeed, the core-hub Adamts1 has been identified as a risk locus for AD [40], and the APOE4 has been specifically associated with the upregulation of multiple Serpina3 genes [41]. This suggests that an innate immune response disequilibrium and thrombus formation are common pathological molecular changes in both acute stroke and AD.

There are some limitations of DEG analysis from prior research [42], and we attempted to address these in our current study. First, we addressed the wide heterogeneity of previous studies (due to variations in microarray platforms, labs, and technicians) by using the 'RemoveBatchEfffect' in limma package to remove unwanted batch effects. Second, while DEGs are heterogeneous across species, only two common DEGs have been previously identified [42]. Clustering based on DEGs therefore provided the ability to determine the appropriateness of analysis based on species; we found that DEG analysis and network analysis were suitable for mice models, but not rats. Finally, as sample-processing conditions varied across studies, we identified reperfusion time as a major confounding factor using WGCNA analysis.

However, our study has many limitations. Data used for analyses were taken from experimental animal models, and results should be cautiously interpretated and revalidated in human tissues. Moreover, the analyses did not consider post-transcriptional and post-translational modifications, and further work combining gene expression, protein, and phosphorylation profiles is needed to more accurately predict molecular changes after cerebral ischemia and reperfusion.

## Conclusion

In conclusion, through integrative analysis of gene expression datasets from GEO, we have identified a reperfusion-independent inflammation module and a reperfusion-dependent thrombo-inflammation module. We have further identified and verified seven new inflammation-related core hubs in brain ischemia, including Zfp36, Rhoj, Nfkbiz, Ms4a6d, Serpina3n, and Tgfbi.

## Materials And Methods

### Building the gene expression compendium of the brain or primary cells

Gene expression profiling array data were downloaded from the Gene Expression Omnibus (GEO) using the terms “cerebral ischemia,” “MCAO,” “brain ischemia,” “cerebral Infarction,” or “ischemic attack.” Microarray analyses using RNA samples from mouse and rat brain were included in our study. The basic characteristics used to identify the studies included first author name, year of publication, dataset, and platform. Characteristics of samples were collected, including groups (contralateral or ipsilateral of MCAO), sampling sites (cortex, ischemic penumbra, hemisphere, ischemic core, striatum), ischemia time, and reperfusion time. Using these criteria, 131 mouse samples and 101 rat samples were ultimately selected, and raw data from individual datasets were downloaded.

RNA data from ex vivo sorted primary microglia, astrocyte, epithelium cell, and macrophage were downloaded from the GEO using the abovementioned terms, by applying oxygen-glucose deprivation (OGD) or MCAO as cerebral ischemia models.

### Combining the study-specific estimates from individual datasets and identification of differentially expressed genes (DEGs)

We combined the study-specific estimates from individual mouse or rat datasets according to the guidelines put forward by Ramasamy [7]. Raw data were normalized by log2 transform, probe IDs were converted to official gene symbols, and any probe that did not map to any official gene symbols was discarded. For official gene symbols with multiple probe IDs within a study, we selected the value with the maximum mean value and discarded any official gene symbol that did not provide valuable information in individual datasets and that was not found in at least one individual dataset. For every official gene symbol, we combined the study-specific estimates across the studies and removed the batch effect using the “removeBatchEffect” function in the limma package. We performed a DE analysis between contralateral samples and ipsilateral samples using the R package “limma.” Genes with an adjusted p-value < 0.05 were identified as DEGs. A gene list of the top 5% upregulated and top 5% downregulated genes of the mouse dataset are provided in Table S2.

For merged microglia dataset, we combined the study-specific estimates from individual datasets using the “removeBatchEffect” function in the limma package. DE analyses of expression profiling by array between contralateral samples and ipsilateral samples were performed using the R package “limma,” and those of expression profiling by high throughput sequencing were performed using the R package “edgeR.” Genes with an adjusted p-value < 0.05, and |log2 fold change| > 1 were identified as DEGs of primary inflammatory cells.

### Weighted gene co-expression network analysis (WGCNA) and identification of core hub-genes.

WGCNA is an R package for weighted correlation network analysis and is a method for describing the correlation patterns among genes across samples. WGCNA can find modules of highly correlated genes, and it can measure the correlation of modules to one another or external traits. DS1-DEGs were input as expression data. Characteristics of samples, including group, sampling sites, ischemic time, and reperfusion time, were input as trait data. A β power was used to increase the gap in the scale-free topology network conversion, where the value of β was 5. TOM value was calculated, and genes were clustered into modules on TOM-based dissimilarity. The minimum module size was 30. Correlation of modules and traits were measured using the “cor” function in R studio (version 4.0.3, 250 Northern Ave, Boston, MA 02210). The correlation of gene module membership and gene trait significance of interested modules was calculated to revalidate the correlation of modules and traits. We calculated the connectivity within interested modules, and genes of the highest 5% connectivity were regarded as WGCNA hub-genes. Hub-genes were overlapped with top 5% DS1-DEGs, and the overlapped genes were identified as core hubs of modules (Table S6).

### Pathway and process enrichment analysis based on metascape

Metascape (http://metascape.org/) is an online tool to combine functional enrichment to leverage independent knowledge bases within one integrated portal [43]. Pathway and process enrichment analysis has been carried out with the following ontology sources: KEGG Pathway, GO Biological Processes, Reactome Gene Sets, Canonical Pathways, CORUM, and WikiPathways. WGCNA module genes were input into the metascape. Terms with a p-value < 0.01, a minimum count of 3, and an enrichment factor > 1.5 were collected and grouped into clusters based on their membership similarities. Sub-trees with a similarity of > 0.3 were considered a cluster. The most statistically significant term within a cluster was chosen to represent the cluster. To further capture the relationships between the terms, a subset of enriched terms has been selected and rendered as a network plot, where terms with a similarity > 0.3 are connected by edges (Figure S4). We selected the terms with the best p-values from each of the 20 clusters, with the constraint that there were no more than 15 terms per cluster and no more than 250 terms in total. Each node represented an enriched term and was colored first by its cluster ID. For clarity, term labels were only shown for one term per cluster.

### Pathway gene signatures analyzed using Gene Set Enrichment Analysis (GSEA)

GSEA is a computational method for exploring whether a priori defined set of genes shows statistically significant, concordant differences between two biological states. GSEA was performed using GSEA software (version v4.1.0 Java Web Start) to find enriched terms predicted to have a correlation with all canonical pathways (including BioCarta, KEGG, PID, Reactome, and WikiPathways) in C2 and biological processes in C5. The gene sets containing less than 15 genes or more than 500 genes were excluded. The phenotype label was set as MCAO vs. controls, and metric for ranking genes is Signal2Noise. The number of permutations was set as 1000 replications. Pathways with a nominal p-value < 0.05 and FDR < 0.25 were considered significantly enriched.

### Gene set variation analysis (GSVA)

GSVA (version 1.38.0) is an open-source software package for R. It provides increased power to detect subtle pathway activity changes over a sample population in comparison to GSEA [44]. Pathway analyses were predominantly performed on canonical pathways in C2 and biological processes in C5 of the molecular signatures database. We applied GSVA using standard settings, as implemented in the GSVA package. Enriched pathways were compared by the "limma" package between MCAO and controls, and those with an adjusted p-value < 0.01 were considered significantly enriched.

### Transient and permanent MCAO mouse model

MCAO was induced with an intraluminal suture to occlude the middle cerebral artery as previously described [45] with some modifications. Briefly, mice were anaesthetized with isoflurane in air with spontaneous respiration. Under the operating microscope (RWD Life Science Co. Ltd.), the common carotid artery (CCA), internal carotid artery (ICA), and external carotid artery (ECA) were exposed through a midline neck incision. The proximal portions of the CCA and ICA were temporarily ligated, and the distal portion of ECA was permanently ligated. A 180-μm silicon-coated nylon suture was induced into the ECA and advanced approximately 9.0 mm beyond the carotid bifurcation to occlude the middle cerebral artery. For transient MCAO, the suture was removed to restore blood flow after 90 min occlusion. For permanent MCAO, the suture stayed in the vessels. The neurological evaluation was performed using the Longa scoring method [46]. Mice undergoing ischemia were rested in the home cage for 24 h. During all surgical procedures, mice were maintained normothermic using a heating blanket. Animals with a Longa's score of 1–3 were sacrificed. Those who died in the first 24 h after surgery and those with subarachnoid hemorrhage at the time of killing were excluded.

### RNA quantification by RT-qPCR

About 20-mg brain tissues from the edematous ischemic hemisphere and ipsilateral hemisphere were immediately extracted and frozen in liquid nitrogen. RNA and proteins were extracted and quantified, similar to the steps mentioned in our previously published articles [47]. For RT-qPCR, Gapdh and Actb were used as reference genes for normalization. All primers are listed in Table S8. Data were analyzed with 5–6 biological replicates and 2–3 technical replicates in each group. The Mann–Whitney U test was used to compare data between MCAO and controls, and data with p-values < 0.05 were considered significantly different.

## Abbreviations

| | |
|---|---|
| **DEGs:** | differentially expressed genes |
| **DE:** | differential expression |
| **WGCNA:** | weighted-gene co-expression network analysis |
| **MCAO:** | middle cerebral artery occlusion |
| **GEO:** | Gene Expression Omnibus |
| **DS1:** | training datasets |
| **DS2:** | validation datasets |
| **AD:** | Alzheimer's disease |
| **PPI:** | protein-protein interaction |
| **GWAS:** | genome-wide association studies |
| **SNP:** | Single Nucleotide Polymorphism |
| **MAPK:** | mitogen-activated protein kinase |
| **LAA:** | large artery atherosclerosis |
| **BBB:** | blood-brain barrier |
| **OGD:** | oxygen-glucose deprivation |
| **GSEA:** | Gene Set Enrichment Analysis |
| **GSVA:** | Gene Set Variation Analysis |
| **CCA:** | common carotid artery |
| **ICA:** | internal carotid artery |
| **ECA:** | external carotid artery |

## Declarations

### Ethics approval and consent to participate

The rights and interests of mice met the requirements of the Laboratory Animal Welfare Ethics Committee of Qingdao University (No. 20210401C572420210831043).

**Consent for publication** was not applicable.

### Availability of data and materials

The datasets analyzed during the current study are available in the GEO dataset (https://www.ncbi.nlm.nih.gov/).


### Acknowledgments

We thank LetPub (www.letpub.com) for its linguistic assistance during the preparation of this manuscript.


### Competing interests

The authors declare that they have no competing interests.


### Funding

This work was supported by the National Key R&D Program of China (2019YFC0120000; 2018YFC1312300), the National Natural Science Foundation of China (NSFC: 82071385), and the Key Research and Development Project of Shandong (2019JZZY021010) to Q.W.


### Authors' contributions

W.L. collected and analyzed the data and was a major contributor in writing the manuscript. J.J., Y.X., and Z.C. performed experimental validation. Q.W. reviewed and revised the manuscript and provided financial support. A.X., X.Z., and Z.W. provided experimental guidance and training. T.Q. was a major contributor to picture and chart production.

## References


1. Global Burden of Disease Study C (2015) Global, regional, and national incidence, prevalence, and years lived with disability for 301 acute and chronic diseases and injuries in 188 countries, 1990-2013: a systematic analysis for the Global Burden of Disease Study 2013. Lancet 386 (9995):743-800. doi:10.1016/S0140-6736(15)60692-4
2. Collaborators GBDLRoS, Feigin VL, Nguyen G, Cercy K, Johnson CO, Alam T, Parmar PG, Abajobir AA, Abate KH, Abd-Allah F, Abejie AN, Abyu GY, Ademi Z, Agarwal G, Ahmed MB, Akinyemi RO, Al-Raddadi R, Aminde LN, Amlie-Lefond C, Ansari H, Asayesh H, Asgedom SW, Atey TM, Ayele HT, Banach M, Banerjee A, Barac A, Barker-Collo SL, Barnighausen T, Barregard L, Basu S, Bedi N, Behzadifar M, Bejot Y, Bennett DA, Bensenor IM, Berhe DF, Boneya DJ, Brainin M, Campos-Nonato IR, Caso V, Castaneda-Orjuela CA, Rivas JC, Catala-Lopez F, Christensen H, Criqui MH, Damasceno A, Dandona L, Dandona R, Davletov K, de Courten B, deVeber G, Dokova K, Edessa D, Endres M, Faraon EJA, Farvid MS, Fischer F, Foreman K, Forouzanfar MH, Gall SL, Gebrehiwot TT, Geleijnse JM, Gillum RF, Giroud M, Goulart AC, Gupta R, Gupta R, Hachinski V, Hamadeh RR, Hankey GJ, Hareri HA, Havmoeller R, Hay SI, Hegazy MI, Hibstu DT, James SL, Jeemon P, John D, Jonas JB, Jozwiak J, Kalani R, Kandel A, Kasaeian A, Kengne AP, Khader YS, Khan AR, Khang YH, Khubchandani J, Kim D, Kim YJ, Kivimaki M, Kokubo Y, Kolte D, Kopec JA, Kosen S, Kravchenko M, Krishnamurthi R, Kumar GA, Lafranconi A, Lavados PM, Legesse Y, Li Y, Liang X, Lo WD, Lorkowski S, Lotufo PA, Loy CT, Mackay MT, Abd El Razek HM, Mahdavi M, Majeed A, Malekzadeh R, Malta DC, Mamun AA, Mantovani LG, Martins SCO, Mate KK, Mazidi M, Mehata S, Meier T, Melaku YA, Mendoza W, Mensah GA, Meretoja A, Mezgebe HB, Miazgowski T, Miller TR, Ibrahim NM, Mohammed S, Mokdad AH, Moosazadeh M, Moran AE, Musa KI, Negoi RI, Nguyen M, Nguyen QL, Nguyen TH, Tran TT, Nguyen TT, Anggraini Ningrum DN, Norrving B, Noubiap JJ, O'Donnell MJ, Olagunju AT, Onuma OK, Owolabi MO, Parsaeian M, Patton GC, Piradov M, Pletcher MA, Pourmalek F, Prakash V, Qorbani M, Rahman M, Rahman MA, Rai RK, Ranta A, Rawaf D, Rawaf S, Renzaho AM, Robinson SR, Sahathevan R, Sahebkar A, Salomon JA, Santalucia P, Santos IS, Sartorius B, Schutte AE, Sepanlou SG, Shafieesabet A, Shaikh MA, Shamsizadeh M, Sheth KN, Sisay M, Shin MJ, Shiue I, Silva DAS, Sobngwi E, Soljak M, Sorensen RJD, Sposato LA, Stranges S, Suliankatchi RA, Tabares-Seisdedos R, Tanne D, Nguyen CT, Thakur JS, Thrift AG, Tirschwell DL, Topor-Madry R, Tran BX, Nguyen LT, Truelsen T, Tsilimparis N, Tyrovolas S, Ukwaja KN, Uthman OA, Varakin Y, Vasankari T, Venketasubramanian N, Vlassov VV, Wang W, Werdecker A, Wolfe CDA, Xu G, Yano Y, Yonemoto N, Yu C, Zaidi Z, El Sayed Zaki M, Zhou M, Ziaeian B, Zipkin B, Vos T, Naghavi M, Murray CJL, Roth GA (2018) Global, Regional, and Country-Specific Lifetime Risks of Stroke, 1990 and 2016. The New England journal of medicine 379 (25):2429-2437. doi:10.1056/NEJMoa1804492
3. Lees KR, Bluhmki E, von Kummer R, Brott TG, Toni D, Grotta JC, Albers GW, Kaste M, Marler JR, Hamilton SA, Tilley BC, Davis SM, Donnan GA, Hacke W, Ecass AN, Group Er-PS, Allen K, Mau J, Meier D, del Zoppo G, De Silva DA, Butcher KS, Parsons MW, Barber PA, Levi C, Bladin C, Byrnes G (2010) Time to treatment with intravenous alteplase and outcome in stroke: an updated pooled analysis of ECASS, ATLANTIS, NINDS, and EPITHET trials. Lancet 375 (9727):1695-1703. doi:10.1016/S0140-6736(10)60491-6
4. Mizuma A, You JS, Yenari MA (2018) Targeting Reperfusion Injury in the Age of Mechanical Thrombectomy. Stroke 49 (7):1796-1802. doi:10.1161/STROKEAHA.117.017286
5. Petrovic-Djergovic D, Goonewardena SN, Pinsky DJ (2016) Inflammatory Disequilibrium in Stroke. Circulation research 119 (1):142-158. doi:10.1161/CIRCRESAHA.116.308022
6. McBride DW, Zhang JH (2017) Precision Stroke Animal Models: the Permanent MCAO Model Should Be the Primary Model, Not Transient MCAO. Translational stroke research. doi:10.1007/s12975-017-0554-2

7. Ramasamy A, Mondry A, Holmes CC, Altman DG (2008) Key issues in conducting a meta-analysis of gene expression microarray datasets. PLoS medicine 5 (9):e184. doi:10.1371/journal.pmed.0050184
8. Malik R, Chauhan G, Traylor M, Sargurupremraj M, Okada Y, Mishra A, Rutten-Jacobs L, Giese AK, van der Laan SW, Gretarsdottir S, Anderson CD, Chong M, Adams HHH, Ago T, Almgren P, Amouyel P, Ay H, Bartz TM, Benavente OR, Bevan S, Boncoraglio GB, Brown RD, Jr., Butterworth AS, Carrera C, Carty CL, Chasman DI, Chen WM, Cole JW, Correa A, Cotlarciuc I, Cruchaga C, Danesh J, de Bakker PIW, DeStefano AL, den Hoed M, Duan Q, Engelter ST, Falcone GJ, Gottesman RF, Grewal RP, Gudnason V, Gustafsson S, Haessler J, Harris TB, Hassan A, Havulinna AS, Heckbert SR, Holliday EG, Howard G, Hsu FC, Hyacinth HI, Ikram MA, Ingelsson E, Irvin MR, Jian X, Jimenez-Conde J, Johnson JA, Jukema JW, Kanai M, Keene KL, Kissela BM, Kleindorfer DO, Kooperberg C, Kubo M, Lange LA, Langefeld CD, Langenberg C, Launer LJ, Lee JM, Lemmens R, Leys D, Lewis CM, Lin WY, Lindgren AG, Lorentzen E, Magnusson PK, Maguire J, Manichaikul A, McArdle PF, Meschia JF, Mitchell BD, Mosley TH, Nalls MA, Ninomiya T, O'Donnell MJ, Psaty BM, Pulit SL, Rannikmae K, Reiner AP, Rexrode KM, Rice K, Rich SS, Ridker PM, Rost NS, Rothwell PM, Rotter JI, Rundek T, Sacco RL, Sakaue S, Sale MM, Salomaa V, Sapkota BR, Schmidt R, Schmidt CO, Schminke U, Sharma P, Slowik A, Sudlow CLM, Tanislav C, Tatlisumak T, Taylor KD, Thijs VNS, Thorleifsson G, Thorsteinsdottir U, Tiedt S, Trompet S, Tzourio C, van Duijn CM, Walters M, Wareham NJ, Wassertheil-Smoller S, Wilson JG, Wiggins KL, Yang Q, Yusuf S, Consortium AF, Cohorts for H, Aging Research in Genomic Epidemiology C, International Genomics of Blood Pressure C, Consortium I, Starnet, Bis JC, Pastinen T, Ruusalepp A, Schadt EE, Koplev S, Bjorkegren JLM, Codoni V, Civelek M, Smith NL, Tregouet DA, Christophersen IE, Roselli C, Lubitz SA, Ellinor PT, Tai ES, Kooner JS, Kato N, He J, van der Harst P, Elliott P, Chambers JC, Takeuchi F, Johnson AD, BioBank Japan Cooperative Hospital G, Consortium C, Consortium E-C, Consortium EP-I, International Stroke Genetics C, Consortium M, Neurology Working Group of the CC, Network NSG, Study UKYLD, Consortium M, Sanghera DK, Melander O, Jern C, Strbian D, Fernandez-Cadenas I, Longstreth WT, Jr., Rolfs A, Hata J, Woo D, Rosand J, Pare G, Hopewell JC, Saleheen D, Stefansson K, Worrall BB, Kittner SJ, Seshadri S, Fornage M, Markus HS, Howson JMM, Kamatani Y, Debette S, Dichgans M (2018) Multiancestry genome-wide association study of 520,000 subjects identifies 32 loci associated with stroke and stroke subtypes. Nature genetics 50 (4):524-537. doi:10.1038/s41588-018-0058-3
9. Network NSG, International Stroke Genetics C (2016) Loci associated with ischaemic stroke and its subtypes (SiGN): a genome-wide association study. The Lancet Neurology 15 (2):174-184. doi:10.1016/S1474-4422(15)00338-5
10. Khasanova LT, Stakhovskaya LV, Koltsova EA, Shamalov NA (2019) [Genetic characteristics of stroke]. Zhurnal nevrologii i psikhiatrii imeni SS Korsakova 119 (12. Vyp. 2):65-72. doi:10.17116/jnevro201911912265
11. Pluta R, Ulamek-Koziol M, Januszewski S, Czuczwar SJ (2020) Shared Genomic and Proteomic Contribution of Amyloid and Tau Protein Characteristic of Alzheimer's Disease to Brain Ischemia. International journal of molecular sciences 21 (9). doi:10.3390/ijms21093186
12. Cahoy JD, Emery B, Kaushal A, Foo LC, Zamanian JL, Christopherson KS, Xing Y, Lubischer JL, Krieg PA, Krupenko SA, Thompson WJ, Barres BA (2008) A transcriptome database for astrocytes, neurons, and oligodendrocytes: a new resource for understanding brain development and function. The Journal of neuroscience : the official journal of the Society for Neuroscience 28 (1):264-278. doi:10.1523/JNEUROSCI.4178-07.2008
13. Albright AV, Gonzalez-Scarano F (2004) Microarray analysis of activated mixed glial (microglia) and monocyte-derived macrophage gene expression. Journal of neuroimmunology 157 (1-2):27-38. doi:10.1016/j.jneuroim.2004.09.007
14. Stoll G, Nieswandt B (2019) Thrombo-inflammation in acute ischaemic stroke - implications for treatment. Nature reviews Neurology 15 (8):473-481. doi:10.1038/s41582-019-0221-1
15. Nieswandt B, Watson SP (2003) Platelet-collagen interaction: is GPVI the central receptor? Blood 102 (2):449-461. doi:10.1182/blood-2002-12-3882
16. Lyu C, Chen Y, Zhu M, Jin X, Liu P, Zheng Z, Li C, Zhu F, Hu X, Wang F, Li W, Wang W (2015) [Association of ADAMTS-1 gene polymorphisms with ischemic stroke caused by large artery atherosclerosis]. Zhonghua yi xue yi chuan xue za zhi = Zhonghua yixue yichuanxue zazhi = Chinese journal of medical genetics 32 (6):844-848. doi:10.3760/cma.j.issn.1003-9406.2015.06.021
17. Pelisek J, Deutsch L, Ansel A, Pongratz J, Stadlbauer T, Gebhard H, Matevossian E, Eckstein HH (2017) Expression of a metalloproteinase family of ADAMTS in human vulnerable carotid lesions. Journal of cardiovascular medicine 18 (1):10-18. doi:10.2459/JCM.0000000000000254
18. Wang L, Zhou C, Wang Z, Liu J, Jing Z, Zhang Z, Wang Y (2011) Dynamic variation of genes profiles and pathways in the hippocampus of ischemic mice: a genomic study. Brain research 1372:13-21. doi:10.1016/j.brainres.2010.11.099
19. Rahimian R, Beland LC, Kriz J (2018) Galectin-3: mediator of microglia responses in injured brain. Drug discovery today 23 (2):375-381. doi:10.1016/j.drudis.2017.11.004
20. Shirakawa K, Endo J, Kataoka M, Katsumata Y, Yoshida N, Yamamoto T, Isobe S, Moriyama H, Goto S, Kitakata H, Hiraide T, Fukuda K, Sano M (2018) IL (Interleukin)-10-STAT3-Galectin-3 Axis Is Essential for Osteopontin-Producing Reparative Macrophage Polarization After Myocardial Infarction. Circulation 138 (18):2021-2035. doi:10.1161/CIRCULATIONAHA.118.035047
21. Venkatraman A, Hardas S, Patel N, Singh Bajaj N, Arora G, Arora P (2018) Galectin-3: an emerging biomarker in stroke and cerebrovascular diseases. European journal of neurology 25 (2):238-246. doi:10.1111/ene.13496
22. Li Y, Dammer EB, Zhang-Brotzge X, Chen S, Duong DM, Seyfried NT, Kuan CY, Sun YY (2017) Osteopontin Is a Blood Biomarker for Microglial Activation and Brain Injury in Experimental Hypoxic-Ischemic Encephalopathy. eNeuro 4 (1). doi:10.1523/ENEURO.0253-16.2016
23. Son YO, Kim HE, Choi WS, Chun CH, Chun JS (2019) RNA-binding protein ZFP36L1 regulates osteoarthritis by modulating members of the heat shock protein 70 family. Nature communications 10 (1):77. doi:10.1038/s41467-018-08035-7
24. Galloway A, Saveliev A, Lukasiak S, Hodson DJ, Bolland D, Balmanno K, Ahlfors H, Monzon-Casanova E, Mannurita SC, Bell LS, Andrews S, Diaz-Munoz MD, Cook SJ, Corcoran A, Turner M (2016) RNA-binding proteins ZFP36L1 and ZFP36L2 promote cell quiescence. Science 352 (6284):453-459. doi:10.1126/science.aad5978
25. Makita S, Takatori H, Nakajima H (2021) Post-Transcriptional Regulation of Immune Responses and Inflammatory Diseases by RNA-Binding ZFP36 Family Proteins. Frontiers in immunology 12:711633. doi:10.3389/fimmu.2021.711633

26. Jing Q, Huang S, Guth S, Zarubin T, Motoyama A, Chen J, Di Padova F, Lin SC, Gram H, Han J (2005) Involvement of microRNA in AU-rich element-mediated mRNA instability. Cell 120 (5):623-634. doi:10.1016/j.cell.2004.12.038
27. Tiedje C, Diaz-Munoz MD, Trulley P, Ahlfors H, Laass K, Blackshear PJ, Turner M, Gaestel M (2016) The RNA-binding protein TTP is a global post-transcriptional regulator of feedback control in inflammation. Nucleic acids research 44 (15):7418-7440. doi:10.1093/nar/gkw474
28. Kang JG, Amar MJ, Remaley AT, Kwon J, Blackshear PJ, Wang PY, Hwang PM (2011) Zinc finger protein tristetraprolin interacts with CCL3 mRNA and regulates tissue inflammation. Journal of immunology 187 (5):2696-2701. doi:10.4049/jimmunol.1101149
29. Liang J, Lei T, Song Y, Yanes N, Qi Y, Fu M (2009) RNA-destabilizing factor tristetraprolin negatively regulates NF-kappaB signaling. The Journal of biological chemistry 284 (43):29383-29390. doi:10.1074/jbc.M109.024745
30. Guo H, Jiang Y, Gu Z, Ren L, Zhu C, Yu S, Wei R (2022) ZFP36 protects against oxygen-glucose deprivation/reoxygenation-induced mitochondrial fragmentation and neuronal apoptosis through inhibiting NOX4-DRP1 pathway. Brain research bulletin 179:57-67. doi:10.1016/j.brainresbull.2021.12.003
31. Muta T, Yamazaki S, Eto A, Motoyama M, Takeshige K (2003) IkappaB-zeta, a new anti-inflammatory nuclear protein induced by lipopolysaccharide, is a negative regulator for nuclear factor-kappaB. Journal of endotoxin research 9 (3):187-191. doi:10.1179/096805103125001612
32. Ishiguro-Oonuma T, Ochiai K, Hashizume K, Morimatsu M (2015) The role of IFN-gamma in regulating Nfkbiz expression in epidermal keratinocytes. Biomedical research 36 (2):103-107. doi:10.2220/biomedres.36.103
33. Slowikowski K, Nguyen HN, Noss EH, Simmons DP, Mizoguchi F, Watts GFM, Gurish MF, Brenner MB, Raychaudhuri S (2020) CUX1 and IkappaBzeta (NFKBIZ) mediate the synergistic inflammatory response to TNF and IL-17A in stromal fibroblasts. Proceedings of the National Academy of Sciences of the United States of America 117 (10):5532-5541. doi:10.1073/pnas.1912702117
34. Horber S, Hildebrand DG, Lieb WS, Lorscheid S, Hailfinger S, Schulze-Osthoff K, Essmann F (2016) The Atypical Inhibitor of NF-kappaB, IkappaBzeta, Controls Macrophage Interleukin-10 Expression. The Journal of biological chemistry 291 (24):12851-12861. doi:10.1074/jbc.M116.718825
35. Cui Y, Wan Q (2019) NKT Cells in Neurological Diseases. Frontiers in cellular neuroscience 13:245. doi:10.3389/fncel.2019.00245
36. Katsuoka F, Yamamoto M (2016) Small Maf proteins (MafF, MafG, MafK): History, structure and function. Gene 586 (2):197-205. doi:10.1016/j.gene.2016.03.058
37. von Scheidt M, Zhao Y, de Aguiar Vallim TQ, Che N, Wierer M, Seldin MM, Franzen O, Kurt Z, Pang S, Bongiovanni D, Yamamoto M, Edwards PA, Ruusalepp A, Kovacic JC, Mann M, Bjorkegren JLM, Lusis AJ, Yang X, Schunkert H (2021) Transcription Factor MAFF (MAF Basic Leucine Zipper Transcription Factor F) Regulates an Atherosclerosis Relevant Network Connecting Inflammation and Cholesterol Metabolism. Circulation 143 (18):1809-1823. doi:10.1161/CIRCULATIONAHA.120.050186
38. Huang X, Feng Z, Jiang Y, Li J, Xiang Q, Guo S, Yang C, Fei L, Guo G, Zheng L, Wu Y, Chen Y (2019) VSIG4 mediates transcriptional inhibition of Nlrp3 and Il-1beta in macrophages. Science advances 5 (1):eaau7426. doi:10.1126/sciadv.aau7426
39. Henstridge CM, Hyman BT, Spires-Jones TL (2019) Beyond the neuron-cellular interactions early in Alzheimer disease pathogenesis. Nature reviews Neuroscience 20 (2):94-108. doi:10.1038/s41583-018-0113-1
40. Kunkle BW, Grenier-Boley B, Sims R, Bis JC, Damotte V, Naj AC, Boland A, Vronskaya M, van der Lee SJ, Amlie-Wolf A, Bellenguez C, Frizatti A, Chouraki V, Martin ER, Sleegers K, Badarinarayan N, Jakobsdottir J, Hamilton-Nelson KL, Moreno-Grau S, Olaso R, Raybould R, Chen Y, Kuzma AB, Hiltunen M, Morgan T, Ahmad S, Vardarajan BN, Epelbaum J, Hoffmann P, Boada M, Beecham GW, Garnier JG, Harold D, Fitzpatrick AL, Valladares O, Moutet ML, Gerrish A, Smith AV, Qu L, Bacq D, Denning N, Jian X, Zhao Y, Del Zompo M, Fox NC, Choi SH, Mateo I, Hughes JT, Adams HH, Malamon J, Sanchez-Garcia F, Patel Y, Brody JA, Dombroski BA, Naranjo MCD, Daniilidou M, Eiriksdottir G, Mukherjee S, Wallon D, Uphill J, Aspelund T, Cantwell LB, Garzia F, Galimberti D, Hofer E, Butkiewicz M, Fin B, Scarpini E, Sarnowski C, Bush WS, Meslage S, Kornhuber J, White CC, Song Y, Barber RC, Engelborghs S, Sordon S, Voijnovic D, Adams PM, Vandenberghe R, Mayhaus M, Cupples LA, Albert MS, De Deyn PP, Gu W, Himali JJ, Beekly D, Squassina A, Hartmann AM, Orellana A, Blacker D, Rodriguez-Rodriguez E, Lovestone S, Garcia ME, Doody RS, Munoz-Fernadez C, Sussams R, Lin H, Fairchild TJ, Benito YA, Holmes C, Karamujic-Comic H, Frosch MP, Thonberg H, Maier W, Roshchupkin G, Ghetti B, Giedraitis V, Kawalia A, Li S, Huebinger RM, Kilander L, Moebus S, Hernandez I, Kamboh MI, Brundin R, Turton J, Yang Q, Katz MJ, Concari L, Lord J, Beiser AS, Keene CD, Helisalmi S, Kloszewska I, Kukull WA, Koivisto AM, Lynch A, Tarraga L, Larson EB, Haapasalo A, Lawlor B, Mosley TH, Lipton RB, Solfrizzi V, Gill M, Longstreth WT, Jr., Montine TJ, Frisardi V, Diez-Fairen M, Rivadeneira F, Petersen RC, Deramecourt V, Alvarez I, Salani F, Ciaramella A, Boerwinkle E, Reiman EM, Fievet N, Rotter JI, Reisch JS, Hanon O, Cupidi C, Andre Uitterlinden AG, Royall DR, Dufouil C, Maletta RG, de Rojas I, Sano M, Brice A, Cecchetti R, George-Hyslop PS, Ritchie K, Tsolaki M, Tsuang DW, Dubois B, Craig D, Wu CK, Soininen H, Avramidou D, Albin RL, Fratiglioni L, Germanou A, Apostolova LG, Keller L, Koutroumani M, Arnold SE, Panza F, Gkatzima O, Asthana S, Hannequin D, Whitehead P, Atwood CS, Caffarra P, Hampel H, Quintela I, Carracedo A, Lannfelt L, Rubinsztein DC, Barnes LL, Pasquier F, Frolich L, Barral S, McGuinness B, Beach TG, Johnston JA, Becker JT, Passmore P, Bigio EH, Schott JM, Bird TD, Warren JD, Boeve BF, Lupton MK, Bowen JD, Proitsi P, Boxer A, Powell JF, Burke JR, Kauwe JSK, Burns JM, Mancuso M, Buxbaum JD, Bonuccelli U, Cairns NJ, McQuillin A, Cao C, Livingston G, Carlson CS, Bass NJ, Carlsson CM, Hardy J, Carney RM, Bras J, Carrasquillo MM, Guerreiro R, Allen M, Chui HC, Fisher E, Masullo C, Crocco EA, DeCarli C, Bisceglio G, Dick M, Ma L, Duara R, Graff-Radford NR, Evans DA, Hodges A, Faber KM, Scherer M, Fallon KB, Riemenschneider M, Fardo DW, Heun R, Farlow MR, Kolsch H, Ferris S, Leber M, Foroud TM, Heuser I, Galasko DR, Giegling I, Gearing M, Hull M, Geschwind DH, Gilbert JR, Morris J, Green RC, Mayo K, Growdon JH, Feulner T, Hamilton RL, Harrell LE, Drichel D, Honig LS, Cushion TD, Huentelman MJ, Hollingworth P, Hulette CM, Hyman BT, Marshall R, Jarvik GP, Meggy A, Abner E, Menzies GE, Jin LW, Leonenko G, Real LM, Jun GR, Baldwin CT, Grozeva D, Karydas A, Russo G, Kaye JA, Kim R, Jessen F, Kowall NW, Vellas B, Kramer JH, Vardy E, LaFerla FM, Jockel KH, Lah JJ, Dichgans M, Leverenz JB, Mann D, Levey AI, Pickering-Brown S, Lieberman AP, Klopp N, Lunetta KL, Wichmann HE, Lyketsos CG, Morgan K, Marson DC, Brown K, Martiniuk F, Medway C, Mash DC, Nothen MM, Masliah E, Hooper NM, McCormick WC, Daniele A, McCurry SM, Bayer A, McDavid AN, Gallacher J, McKee AC, van den Bussche H, Mesulam M, Brayne C, Miller BL, Riedel-Heller S, Miller CA, Miller JW, Al-Chalabi A, Morris JC, Shaw CE, Myers AJ, Wiltfang J, O'Bryant S, Olichney JM, Alvarez V, Parisi JE, Singleton AB, Paulson HL, Collinge J, Perry WR, Mead S, Peskind E, Cribbs DH, Rossor M, Pierce A, Ryan NS, Poon WW, Nacmias B, Potter H, Sorbi S, Quinn JF, Sacchinelli E, Raj A, Spalletta G, Raskind M, Caltagirone C, Bossu P, Orfei MD, Reisberg B, Clarke R, Reitz C, Smith AD, Ringman JM, Warden D, Roberson ED, Wilcock G, Rogaeva E, Bruni AC, Rosen HJ,

Gallo M, Rosenberg RN, Ben-Shlomo Y, Sager MA, Mecocci P, Saykin AJ, Pastor P, Cuccaro ML, Vance JM, Schneider JA, Schneider LS, Slifer S, Seeley WW, Smith AG, Sonnen JA, Spina S, Stern RA, Swerdlow RH, Tang M, Tanzi RE, Trojanowski JQ, Troncoso JC, Van Deerlin VM, Van Eldik LJ, Vinters HV, Vonsattel JP, Weintraub S, Welsh-Bohmer KA, Wilhelmsen KC, Williamson J, Wingo TS, Woltjer RL, Wright CB, Yu CE, Yu L, Saba Y, Pilotto A, Bullido MJ, Peters O, Crane PK, Bennett D, Bosco P, Coto E, Boccardi V, De Jager PL, Lleo A, Warner N, Lopez OL, Ingelsson M, Deloukas P, Cruchaga C, Graff C, Gwilliam R, Fornage M, Goate AM, Sanchez-Juan P, Kehoe PG, Amin N, Ertekin-Taner N, Berr C, Debette S, Love S, Launer LJ, Younkin SG, Dartigues JF, Corcoran C, Ikram MA, Dickson DW, Nicolas G, Campion D, Tschanz J, Schmidt H, Hakonarson H, Clarimon J, Munger R, Schmidt R, Farrer LA, Van Broeckhoven C, M COD, DeStefano AL, Jones L, Haines JL, Deleuze JF, Owen MJ, Gudnason V, Mayeux R, Escott-Price V, Psaty BM, Ramirez A, Wang LS, Ruiz A, van Duijn CM, Holmans PA, Seshadri S, Williams J, Amouyel P, Schellenberg GD, Lambert JC, Pericak-Vance MA, Alzheimer Disease Genetics C, European Alzheimer's Disease I, Cohorts for H, Aging Research in Genomic Epidemiology C, Genetic, Environmental Risk in Ad/Defining Genetic P, Environmental Risk for Alzheimer's Disease C (2019) Genetic meta-analysis of diagnosed Alzheimer's disease identifies new risk loci and implicates Abeta, tau, immunity and lipid processing. Nature genetics 51 (3):414-430. doi:10.1038/s41588-019-0358-2

41. Zhao N, Ren Y, Yamazaki Y, Qiao W, Li F, Felton LM, Mahmoudiandehkordi S, Kueider-Paisley A, Sonoustoun B, Arnold M, Shue F, Zheng J, Attrebi ON, Martens YA, Li Z, Bastea L, Meneses AD, Chen K, Thompson JW, St John-Williams L, Tachibana M, Aikawa T, Oue H, Job L, Yamazaki A, Liu CC, Storz P, Asmann YW, Ertekin-Taner N, Kanekiyo T, Kaddurah-Daouk R, Bu G (2020) Alzheimer's Risk Factors Age, APOE Genotype, and Sex Drive Distinct Molecular Pathways. Neuron 106 (5):727-742 e726. doi:10.1016/j.neuron.2020.02.034
42. Zhou H, Qiu Z, Gao S, Chen Q, Li S, Tan W, Liu X, Wang Z (2016) Integrated Analysis of Expression Profile Based on Differentially Expressed Genes in Middle Cerebral Artery Occlusion Animal Models. International journal of molecular sciences 17 (5). doi:10.3390/ijms17050776
43. Zhou Y, Zhou B, Pache L, Chang M, Khodabakhshi AH, Tanaseichuk O, Benner C, Chanda SK (2019) Metascape provides a biologist-oriented resource for the analysis of systems-level datasets. Nature communications 10 (1):1523. doi:10.1038/s41467-019-09234-6
44. Hanzelmann S, Castelo R, Guinney J (2013) GSVA: gene set variation analysis for microarray and RNA-seq data. BMC bioinformatics 14:7. doi:10.1186/1471-2105-14-7
45. Smith HK, Russell JM, Granger DN, Gavins FN (2015) Critical differences between two classical surgical approaches for middle cerebral artery occlusion-induced stroke in mice. Journal of neuroscience methods 249:99-105. doi:10.1016/j.jneumeth.2015.04.008
46. Guo P, Jin Z, Wu H, Li X, Ke J, Zhang Z, Zhao Q (2019) Effects of irisin on the dysfunction of blood-brain barrier in rats after focal cerebral ischemia/reperfusion. Brain and behavior 9 (10):e01425. doi:10.1002/brb3.1425
47. Lv W, Deng B, Duan W, Li Y, Song X, Ji Y, Li Z, Liu Y, Wang X, Li C (2019) FGF9 alters the Wallerian degeneration process by inhibiting Schwann cell transformation and accelerating macrophage infiltration. Brain research bulletin 152:285-296. doi:10.1016/j.brainresbull.2019.06.011

## Tables

Table 1. mRNA expression of core hub-genes in transient MCAO (tmcao) and permanent MCAO (pmcao).

| Hub-genes | Normalized by Actb | | | Normalized by Gapdh | | | Normalized by Actb | | | Normaliz |
|---|---|---|---|---|---|---|---|---|---|---|
| | control | tmcao | p-value | control | tmcao | p-value | control | pmcao | p-value | control |
| Zfp36 | 1.71±0.658 | 1.387±0.446 | 0.28293 | 1.267±0.267 | 1.349±0.207 | 0.49651 | 2.187±0.735 | 6.801±1.866 | 0.02593 | 2.135±0. |
| Rhoj | 1.088±0.077 | 4.804±0.903 | 0.00001 | 1.258±0.155 | 7.698±1.829 | 0.00005 | 1.271±0.312 | 8.677±2.235 | 0.00265 | 1.785±0. |
| Nfkbiz | 1.122±0.153 | 4.121±1.085 | 0.00066 | 1.249±0.282 | 5.496±1.82 | 0.01004 | 1.368±0.365 | 10.57±1.415 | 0.00002 | 1.138±0. |
| Adamts1 | 1.221±0.256 | 4.924±1.406 | 0.01727 | 1.116±0.171 | 4.419±1.017 | 0.00010 | 2.699±1.146 | 30.569±13.47 | 0.01377 | 3.178±1. |
| Lgals3 | 1.264±0.334 | 37.31±7.958 | 0.00002 | 1.206±1.206 | 35.76±12.58 | 0.00002 | 1.523±0.778 | 19.15±5.679 | 0.00021 | 1.131±0. |
| Spp1 | 1.103±0.215 | 13.48±3.094 | 0.00004 | 1.017±0.081 | 13.78±4.62 | 0.01707 | 1.222±0.554 | 12.29±3.685 | 0.00113 | 0.944±0. |
| Ms4a6d | 1.945±0.737 | 34.63±9.465 | 0.00001 | 1.721±0.385 | 55.18±20.47 | 0.00000 | 0.825±0.268 | 8.485±1.417 | 0.00564 | 1.218±0. |
| Serpina3n | 5.078±2.648 | 17.61±7.628 | 0.01449 | 3.425±1.694 | 39.53±23.31 | 0.00451 | 2.142±0.111 | 6.104±1.833 | 0.05032 | 2.125±0. |
| Tgfbi | 2.321±0.898 | 2.002±0.582 | 1.00000 | 1.825±0.455 | 2.098±0.551 | 0.88836 | 1.537±0.476 | 7.816±3.526 | 0.20600 | 1.449±0. |
| Rgs9 | 2.186±0.624 | 0.232±0.074 | 0.00098 | 2.519±0.926 | 0.239±0.045 | 0.00698 | 4.221±1.629 | 1.972±1.393 | 0.80780 | 4.987±1. |
| Gpr34 | 2.193±0.625 | 0.232±0.074 | 0.00098 | 2.667±0.745 | 5.291±1.773 | 0.26045 | 1.397±0.322 | 0.527±0.131 | 0.01574 | 1.369±0. |
| Myoc | 2.205±0.644 | 2.696±1.263 | 0.79875 | 1.246±0.226 | 0.594±0.099 | 0.05186 | 1.126±0.162 | 3.383±1.057 | 0.00288 | 1.282±0. |
| Crybb1 | 1.196±0.212 | 1.083±0.485 | 0.08042 | 1.089±0.138 | 0.685±0.114 | 0.04257 | 1.507±0.33 | 0.821±0.209 | 0.19323 | 1.674±0. |
| Rhobtb2 | 3.519±1.268 | 1.302±0.533 | 0.34700 | 2.085±0.659 | 0.388±0.084 | 0.03742 | 3.225±1.427 | 2.549±0.711 | 0.43587 | 3.842±1. |

## Figures

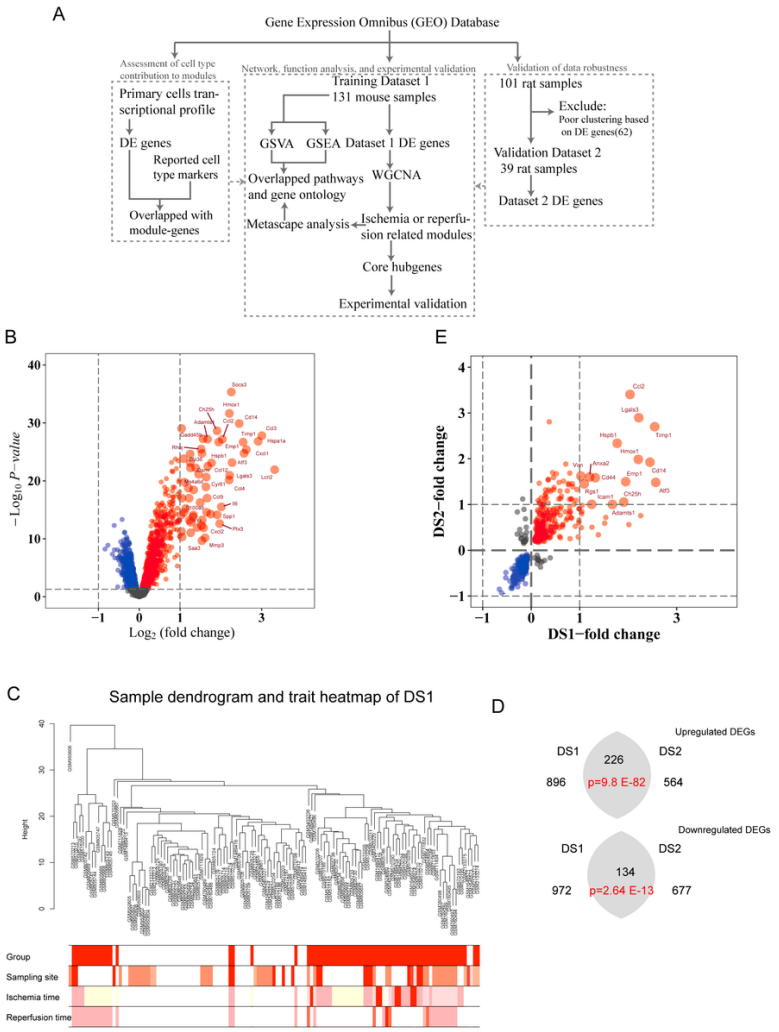


## Figure 1

**Integration, validation, and DE analysis of data from brain ischemia samples**. **A** Workflow of the integrated analysis for brain ischemia in GEO datasets. Data from mouse brain samples were identified as training DS1. The robustness of DS1 data was validated by rat brain samples DS2. DE analysis and WGCNA analysis of DS1 were used to explore phenotype related gene modules and hub-genes. The expression of unreported and part of the known human stroke susceptibility genes related to hub-genes was experimentally validated. Module functions were clarified using GSEA, GSVA, and metascape analysis. Reported cell type markers and primary cell transcriptional profile in brain ischemia were used to assess the cell type contribution to module gene profile. **B** Volcano plot of DEGs in DS1. Genes with p-value < 0.05 and with Log2(fold change) > 1 were labeled. **C** Clustering analysis and traits of all samples in DS1. Colors range from light to dark red: Group – control, MCAO; Sample sites – cortex, penumbra, CA1 region of hippocampus, hemisphere, core, and striatum; ischemia time – 0 h, 0.17 h, 0.5 h, 0.75 h, 1 h, 2 h, 6 h; reperfusion time – 0 h, 2 h, 3 h, 8 h, 24 h, 48 h, 72 h. **D** The overlap of upregulated DEGs and downregulated DEGs in DS1 and DS2 (hypergeometric test), respectively. **E** Scatter plot of gene expression in DS1-DEGs and DS2-DEGs. Genes with fold change > 1 in both DS1 and DS2 were labeled.

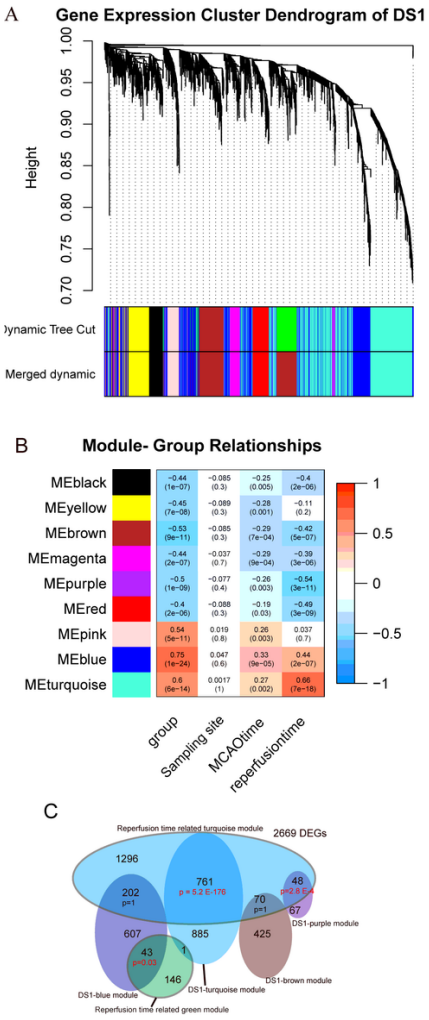


## Figure 2

**Mapping genetic modules of brain ischemia. A** Gene clustering of DS1 on 'TOM'-based dissimilarity. Genes with similar dissimilarity were set into the same module using the function 'cuttreeDynamic.' Modules with similarity > 0.8 based on 'eigengenes' were merged. **B** Heatmap of relationships between modules and group; the values were set as the 'correlation coefficient (p-value).' **C** The overlap of reperfusion-related module genes and DS1-modules (hypergeometric test).

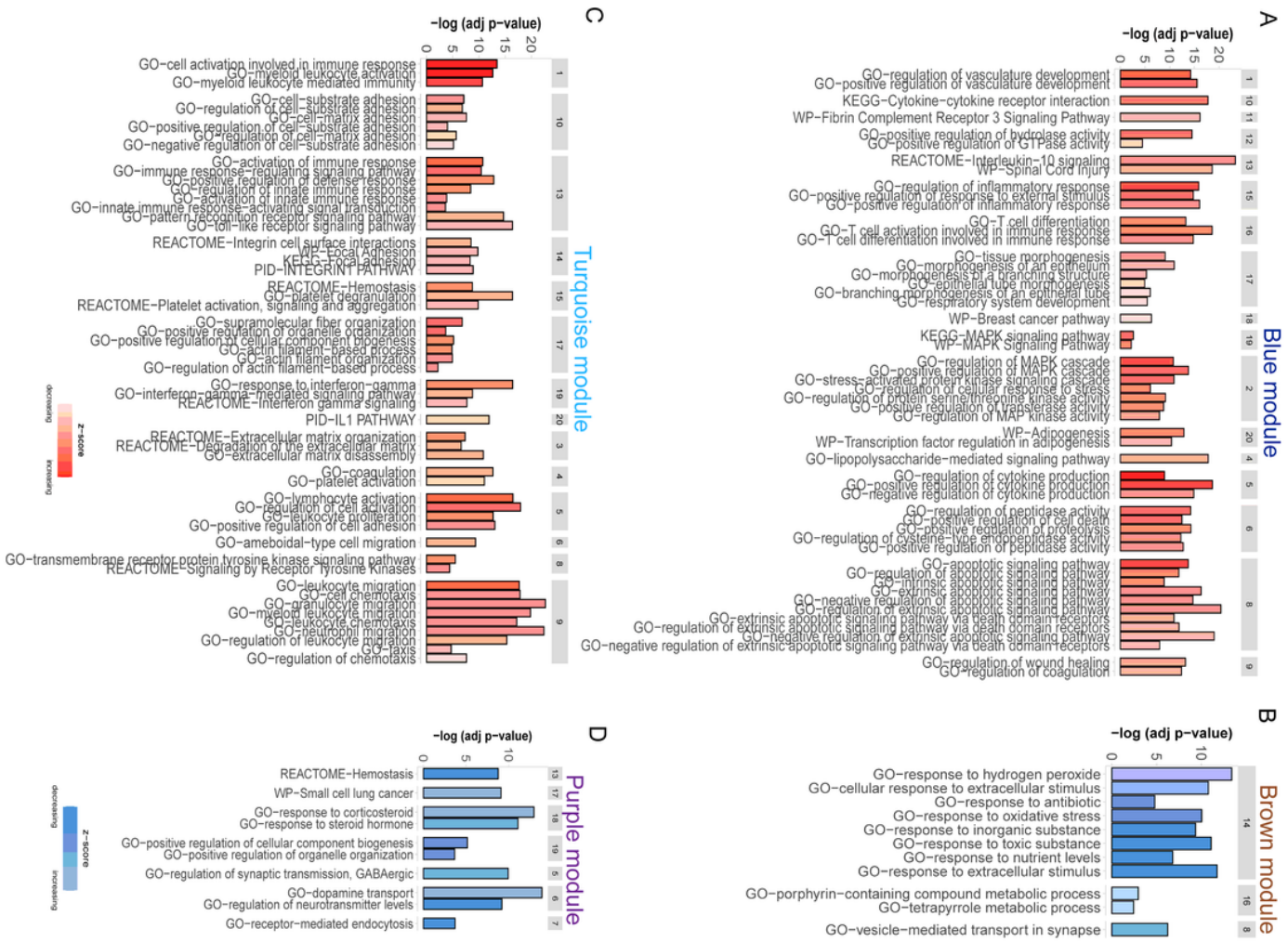


**Figure 3**

**Identification of module genes' pathway and process enrichment. A–D** Bar plots of the module genes' related pathway and process. Terms with similarity > 0.3 are considered a cluster, which range from 1 to 20. Z-scores indicate whether a pathway or process is more likely to decrease or increase. Z-score =

.

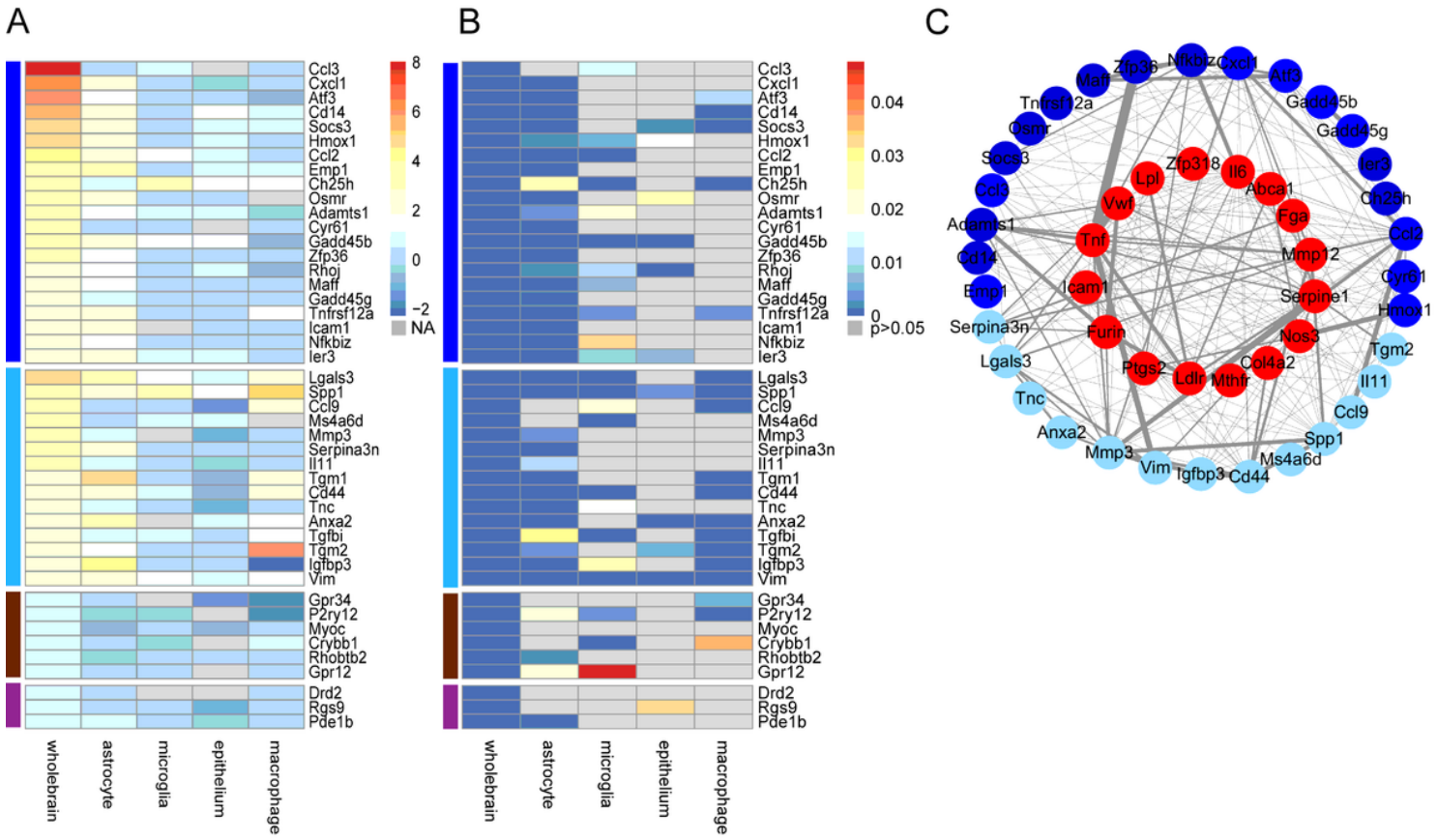


**Figure 4**

Heatmap of log2 fold change **A** and p value **B** of core hubs in whole brain and primary cells. **C** PPI network of core hubs and known human stroke susceptibility genes based on the STRING network. The edges' thickness represents the experimentally determined interactions' scores. The red, blue, and turquoise dots represent the known human stroke susceptibility genes, the blue module core hubs, and the turquoise module core hubs, respectively.

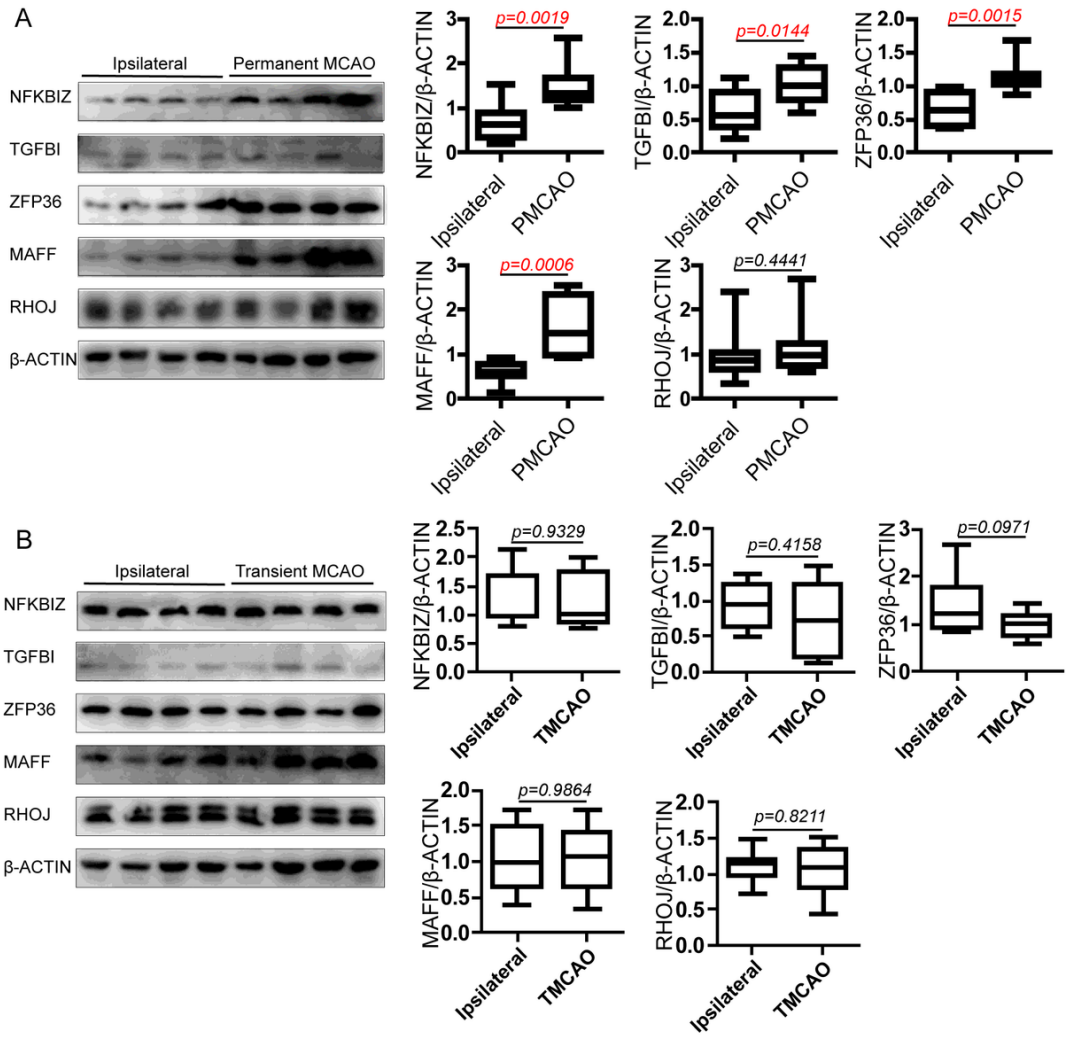


**Figure 5**

Protein expression analysis of ipsilateral and ischemia brains from permanent MCAO **A** and transient MCAO **B**. (n=4 for each group, three independent tests were performed by Western Blot)

## Supplementary Files

This is a list of supplementary files associated with this preprint. Click to download.

- Figurelegendsofsupplementarymaterials.docx
- TableS1studies.docx
- TableS2DEGs.docx
- TableS3DEGsinDS1DS2.docx
- TableS4cellspecificmarkers.docx
- TableS5pathways.docx
- TableS6hubgenes.docx
- TableS7hubgenecellexpression.docx
- TableS8Primers.docx
- TableS9brainischemicsusceptiblegenes.docx